IOPscience iopscience.iop.org

Home Search Collections Journals About Contact us My IOPscience

Local structure in Ti–Hf–Ni metallic glasses and its evolution with hydrogenation

This article has been downloaded from IOPscience. Please scroll down to see the full text article.

2005 J. Phys.: Condens. Matter 17 1481

(http://iopscience.iop.org/0953-8984/17/10/005)

View the table of contents for this issue, or go to the journal homepage for more

Download details:
IP Address: 129.252.86.83
The article was downloaded on 27/05/2010 at 20:25

Please note that terms and conditions apply.

INSTITUTE OF PHYSICS PUBLISHING JOURNAL OF PHYSICS: CONDENSED MATTER

J. Phys.: Condens. Matter **17** (2005) 1481–1492 doi:10.1088/0953-8984/17/10/005

Local structure in Ti–Hf–Ni metallic glasses and its evolution with hydrogenation

A Sadoc[1,2], V T Huett[3] and K F Kelton[3]

[1] Laboratoire de Physique des Matériaux et des Surfaces, Université de Cergy-Pontoise, Neuville sur Oise, 95031 Cergy-Pontoise, Cedex, France
[2] Laboratoire pour l'Utilisation du Rayonnement Electromagnétique, CNRS, MENESR, CEA, Bâtiment 209D, Centre Universitaire Paris-Sud, BP 34, 91898 Orsay Cedex, France
[3] Department of Physics, Washington University, St Louis, MO 63130, USA

E-mail: Anne.Sadoc@lpms.u-cergy.fr

Received 19 November 2004, in final form 26 January 2005
Published 25 February 2005
Online at stacks.iop.org/JPhysCM/17/1481

Abstract

The effect of hydrogenation on the local structure of a $Ti_{25}Hf_{50}Ni_{25}$ amorphous alloy was studied by extended x-ray absorption fine structure (EXAFS) measurements. The samples were loaded to different hydrogen-to-metal ratios, H/M, 1.2 and 1.4. For the non-hydrogenated alloy, the local structure was found to be different from that in the crystalline Ti–Hf–Ni phase. A new icosahedral ordering, similar to that in the Ti_2Ni crystal, is identified around the nickel atoms. Upon hydrogenation, little change is observed in the environment of the nickel atoms. As in the 3/2 phase and in the Ti–Zr–Ni alloys, the perturbation of the local structure with hydrogenation concerns mainly the environments of hafnium (zirconium) and titanium atoms. This indicates that the hydrogen atoms sit preferentially near hafnium (zirconium) and titanium neighbours. Moreover, a drastic decrease of the disorder parameter for the Hf–Ti correlation could be explained by a stiffening of the structure of the glass, possibly due to the formation of a hydrogen network.

(Some figures in this article are in colour only in the electronic version)

1. Introduction

One way to reduce emissions from internal combustion engines is to use cars that run on an electric motor. A promising technology is the fuel cell, which generates electricity by oxidizing molecular hydrogen, producing only heat and water as by-products. Hydrogen storage can be accomplished, in particular, in metal hydrides where the hydrogen is stored in interstitial sites and induces no structure change, so that it is more likely to be reversible at a reasonable temperature. In particular, Ti-based quasicrystals (QCs) and related crystals might be excellent materials for hydrogen storage because of their high number of tetrahedral

 © 2005 IOP Publishing Ltd Printed in the UK

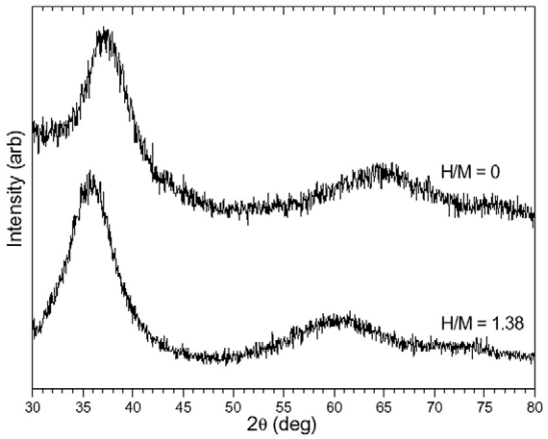

Figure 1. X-ray diffraction pattern of the $Ti_{25}Hf_{50}Ni_{25}$ amorphous samples.

sites suitable for interstitial hydrogen and their favourable hydrogen chemistry. It has been shown that Ti–Zr–Ni and Ti–Hf–Ni alloys, quasicrystals or approximants, can absorb more than two hydrogen atoms for each metallic atom, making them candidates for novel hydrogen storage materials [1–4]. Approximants are crystalline phases with atomic structures related to those of quasicrystals [5]. They can be obtained by the 'cut and projection' method, where the real three-dimensional (3D) space is generated by a 3D cut of a 6D periodic lattice with a rational slope obtained by replacing the golden mean, $\tau = (1 + \sqrt{5})/2$, by one of its rational approximants p/q. The p/q cubic approximants of a given quasicrystal follow a Fibonacci sequence of p/q rational fractions, with p/q, the ratio of consecutive Fibonacci numbers, becoming ever closer to τ: $1/1, 2/1, 3/2, \ldots$.

Now, it is also possible to store hydrogen in Ti–Hf–Ni amorphous alloys. In fact, the study of hydrogen absorption by amorphous alloys has interested scientists for many years [6]. Like crystalline Ti–Hf–Ni, but unlike Ti–Zr–Ni, a $Ti_{25}Hf_{50}Ni_{25}$ amorphous alloy can be loaded without the formation of any detectable crystal hydride phase, detrimental to hydrogen cycling, as shown by the x-ray diffraction patterns in figure 1, where typical amorphous halo-patterns are observed. To improve our understanding of the mechanism of hydrogen absorption in metal–hydrogen systems, one must have a good knowledge of the local structure.

The extended x-ray absorption fine structure (EXAFS) experiment is a convenient method for probing the structure of matter at the atomic and nanometre scales. Although, like x-ray diffraction, EXAFS is not directly sensitive to the presence of hydrogen, it has allowed the study of the average change in local order induced by hydrogen in Ti–Zr–Ni alloys, icosahedral quasicrystal and approximants [7, 8], and also in the $3/2$ approximant Ti–Hf–Ni [9]. The crystalline and quasicrystalline Ti–Zr–Ni phases have different long range structural order, but they present a similar local icosahedral order that also exists in the $3/2$ Ti–Hf–Ni alloys, even around zirconium/hafnium atoms. Open questions still exist, such as does this local icosahedral order also exist in the amorphous Ti–Hf–Ni phase? Moreover, to advance the understanding of hydrogenation, one also needs information about the localization of hydrogen atoms in the alloys. Therefore, we have undertaken an EXAFS study of the evolution of the short range ordering as a function of the hydrogen content in amorphous Ti–Hf–Ni alloys. Preliminary results were reported previously [10, 11].

The paper is organized as follows. In section 2, the experimental methods and the EXAFS analysis are described in detail. A structural model of the $1/1$ approximant Ti–Zr–Ni phase

(W phase) and of the 3/2 approximant Ti–Hf–Ni is described in section 3. This model is the starting point for determining the local order in the amorphous alloy, and in section 4 it is compared with the environments in the approximants. In section 5, we study the hydrogen locations in the hydrogenated amorphous alloy before comparing them with the locations in the approximants and quasicrystals. A summary and conclusion are presented in section 6.

2. Methods

2.1. Experimental details

Samples of $Ti_{25}Hf_{50}Ni_{25}$, an amorphous phase, and of $Ti_{40}Hf_{40}Ni_{20}$, a 3/2 approximant phase, were prepared and characterized at Washington University [4, 12]. Alloy ingots of the desired composition were first produced by arc-melting mixtures of the pure elements on a water-cooled copper hearth in a high-purity argon atmosphere. These ingots were subsequently melted and quenched in an argon atmosphere onto a rotating copper wheel to produce ribbons. The amorphous samples were loaded at 250 °C with hydrogen from the gas phase to a hydrogen-to-metal-atom ratios, H/M, of 1.2 and 1.4 and compared to the approximant alloy loaded to H/M = 0.8, 1.2, 1.4 and 1.7. Gas-phase hydrogenation studies were made using a computer-controlled modified Sievert's apparatus [13]. The values of H/M were determined from the mass change after hydrogenation. Prior to exposure to hydrogen, the samples were first plasma etched in argon and coated with a thin layer of palladium (15–30 nm). The removal of the oxide layer by plasma etching, followed by the vapour deposition of a thin layer of palladium, substantially enhances the rate of hydrogen absorption [14]. The phase microstructures of the samples were checked by x-ray diffraction and transmission electron microscopy.

The EXAFS experiments were performed on powdered samples sieved below 50 μm, except for the non-hydrogenated amorphous ribbon, which was impossible to crush and grind. They were carried out at the Laboratoire pour l'Utilisation du Rayonnement Electromagnétique (LURE, Orsay) using the DCI synchrotron radiation facility on the experimental station EXAFS 13. The x-ray absorption spectra at the Ti and Ni K edges and Hf L_{III} edge (4966, 8331 and 9560 eV respectively) were collected in transmission mode, at low temperature (10 K) using an Si(111) or Si(331) double-crystal monochromator or channel-cut single-crystal monochromator. The intensity of the beam before (I_0) and after (I) the sample was measured with the ionization chambers filled with air. For reference samples and for energy calibration of the EXAFS apparatus, titanium, nickel and hafnium foils were used.

2.2. EXAFS analysis

Standard procedures of normalization and background removal were followed to determine the EXAFS oscillations, χ, versus the energy, E, of the photoelectron from the absorption coefficient, $\ln I_0/I$, using a program package [15, 16]. The data were then converted to momentum space (k-space) using $\hbar^2k^2/2m = E - E_0$, where E_0 is the threshold energy origin and k the photoelectron wavevector. The normalized EXAFS signals, $k^3\chi(k)$, are compared, for the different samples, in figure 2 for the three edges. The signal is noisy for the Ti edge, particularly for the 3/2 sample.

For the non-hydrogenated samples, the spectra of the 3/2 and amorphous samples show, for the Hf and Ti edges, some similarities in the phases and some discrepancies in the intensities. For the Ni edge, they are completely different, as shown in figures 2 and 3. In particular, the oscillations at 6.5 and 8 $Å^{-1}$, which present a single maximum in the amorphous phase, are split in the 3/2 phase, as in the Ti–Zr–Ni alloys, approximant or quasicrystal. These double oscillations can be considered as fingerprints of the 1/1 Ti–Zr–Ni local structure.

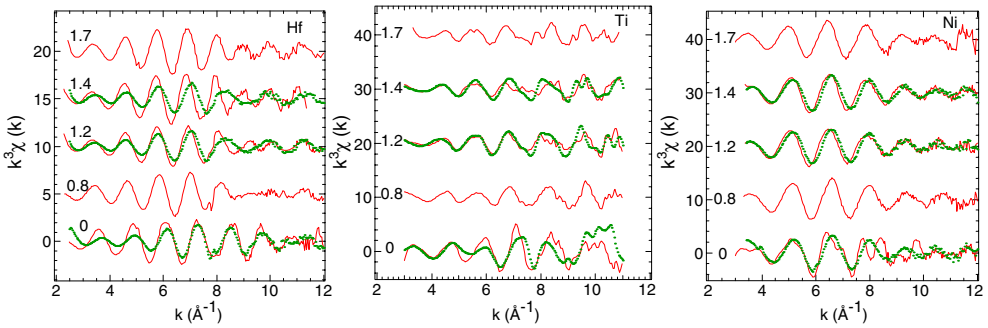

Figure 2. The EXAFS spectra, $k^3\chi(k)$, of the amorphous (dots) and 3/2 (solid curve) Ti–Hf–Ni alloys studied for the Hf L_{III}, Ti K and Ni K edges. From bottom to top, H/M = 0, 0.8, 1.2, 1.4 and 1.7.

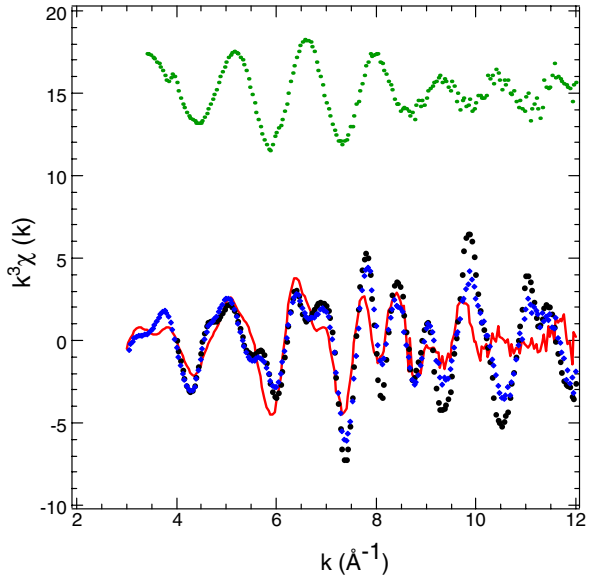

Figure 3. Comparison of the EXAFS spectra for the Ni edge in Ti–Hf–Ni alloys, amorphous (top: dots) and 3/2 (bottom: curve) phases, and in Ti–Zr–Ni alloys, 1/1 (bottom: circles) and icosahedral quasicrystalline (bottom: rhombuses) phases.

For the hydrogenated samples, there is a general tendency for the EXAFS oscillations to shift to lower k-values when H/M increases, according to the simple idea that the interatomic distances increase together with the lattice parameter. For the Ni edge, the spectrum changes little in going from H/M = 0 to 1.2, contrary to the case for the 3/2 phase. The spectra are identical for the two identical H/M concentrations in the amorphous and 3/2 phase (H/M = 1.2 and 1.4), except for a smaller shift toward lower k-values in the amorphous phase. For the Hf edge, the spectra for both the amorphous and 3/2 phases changes by a large amount with hydrogenation, in particular above 8 $Å^{-1}$. The spectra of the two phases differ in the low-k region, showing a smaller shift with hydrogenation for the amorphous alloy. They differ strongly in the high-k region since they have opposite phase at 9 $Å^{-1}$. For the Ti edge, the spectra for the hydrogenated and non-hydrogenated alloys are different. For the amorphous

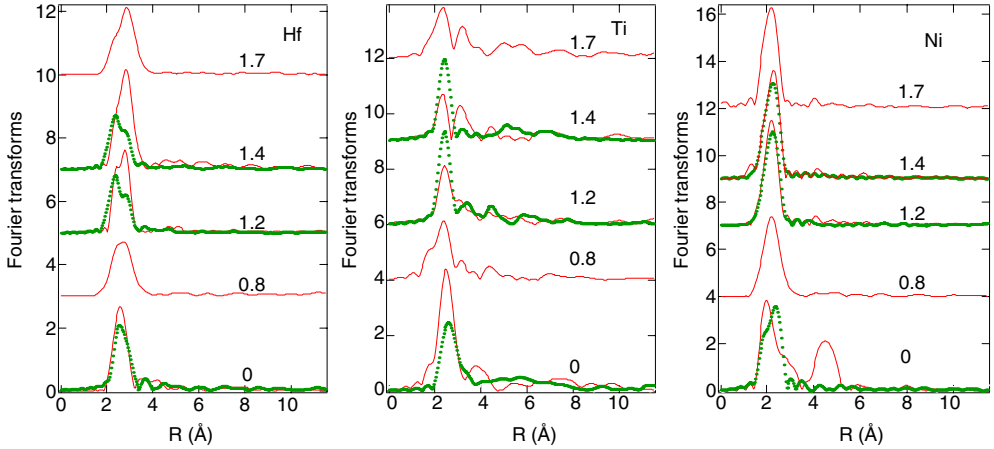

Figure 4. Moduli of the Fourier transforms of the $k^3\chi(k)$ as a function of distance (Å) in amorphous (dots) and 3/2 (solid curve) Ti–Hf–Ni alloys studied for the Hf L_{III}, Ti K and Ni K edges. From bottom to top, H/M = 0, 0.8, 1.2, 1.4 and 1.7.

phase, the spectra are similar up to 9 $Å^{-1}$ for H/M = 1.2 and 1.4. There are some similarities in the low-k region for the amorphous and 3/2 phases for the two H/M concentrations of 1.2 and 1.4, particularly for H/M = 1.2.

The straightforward conclusions are that the EXAFS spectra, and consequently the atomic environments, are not identical in the amorphous and 3/2 alloys, both in the non-hydrogenated samples and the hydrogenated samples.

Therefore, a careful analysis must be made to determine the local structure in the amorphous alloy and its evolution with hydrogenation. Moreover, the local environments appear similar for the two hydrogenated samples of H/M = 1.2 and 1.4, which was not the case for the 3/2 alloy.

The Fourier transforms (FTs) of these data for $k^3\chi(k)$ were obtained within a k window from roughly 3 to 12 $Å^{-1}$ for the Ni and Hf edges and from 3 to 10 $Å^{-1}$ for the Ti edge, where the signal is noisy. The moduli of the FTs, shown in figure 4, are qualitatively similar to the radial distributions of the atoms neighbouring the absorbing atom (Ti, Ni or Hf). However, the peaks are shifted to lower R-distances, because of the phase shifts experienced by the photoelectron while scattering from the potentials of the absorbing atom and nearest neighbours. Due to these phase shifts, the shape of the modulus of the FT does not provide a simple explanation of the environments of the atoms or an interpretation of the evolutions of these environments. Simulations must be done.

The FTs are composed primarily of peaks of first neighbours (1.5–4 Å range), but peaks of second neighbours clearly appear in the 4–5 Å region at the Ni edge in the non-hydrogenated 3/2 alloy. After hydrogenation, this broad band in the 4–5 Å region, corresponding to order in the next nearest neighbour environment, disappears, which may indicate the development of a more disordered structure. At this Ni edge, in the non-hydrogenated 3/2 alloy, the peak of first neighbours is split, with a well-defined component centred at 2 Å (uncorrected for phase shift) and a broad and weaker shoulder from 2.5 to 3.5 Å. In the amorphous alloy, the main peak is centred at 2.35 Å with a shoulder at lower R. No contribution appears in the 2.5–3.5 Å region, so the FTs are very different in the two phases. After hydrogenation, only the main peak survives and the FTs are similar for both phases and for H/M = 1.2 and 1.4, like for the EXAFS signals. At the Ti and Hf edges, the peak of first neighbours is centred

at about 2.5 Å in the non-hydrogenated alloys. At the Hf edge, the main peak broadens with hydrogenation and develops a shoulder. The FTs are similar for the two hydrogenated amorphous alloys. The magnitude of the component at 2.5 Å is higher than that at 3 Å, contrary to the case for the 3/2 phase. At the Ti edge, the magnitude of the main peak increases in the hydrogenated amorphous samples, and the component at 3 Å is small, so these FTs are very different in the two 3/2 and amorphous phases.

To determine the first coordination shell around Ti, Ni or Hf atoms in the different samples, the first peaks between roughly 1.5 and 3.5 Å were back-transformed to k-space. These Fourier-filtered spectra were fitted using the following formula [17], which, in single scattering theories, describes the EXAFS oscillations for a Gaussian distribution of neighbours around a central atom:

$$\chi(k) = -\sum_j \frac{N_j}{kR_j^2} B_j(k) \exp\left(-2\sigma_j^2 k^2 - \frac{2R_j}{\lambda}\right) \sin(2kR_j + 2\delta_1' + \phi_j(k)). \tag{1}$$

The sum is taken over shells with N_j atoms at distances R_j from the absorbing atom. σ_j is the mean square relative displacement of absorber and j backscatter atoms, so that the Debye–Waller factor $\exp(-2\sigma_j^2 k^2)$ is a measure of both static and dynamic disorder in shell j. It arises mainly from structural disorder since the experiments were made at low temperature. $B_j(k)$ and $\phi_j(k)$ are the backscattering amplitude and the phase shift, respectively, experienced by the photoelectron while scattering by the neighbours, δ_1' is the phase shift of the central atom and λ is the electron mean free path. The amplitudes and phase shifts were taken from McKale *et al* [18]. The fitting of the first neighbour peak in the FT was performed in both k- and R-space.

A structural model of the 1/1 approximant Ti–Zr–Ni phase (W phase) [19] was used to simulate the EXAFS spectra of the 3/2 approximant Ti–Hf–Ni, even around the hafnium atom. We will first describe this model before determining the local order in the amorphous alloy and comparing the environments in the 3/2 and amorphous Ti–Hf–Ni alloys.

3. Structural modelling of 1/1 Ti–Zr–Ni and 3/2 Ti–Hf–Ni approximant phases

The refined structure of the W phase (1/1 approximant) of the Ti–Zr–Ni phase was based on x-ray and neutron diffraction measurements [20] and *ab initio* calculations [19]. The basic cluster is a Bergman-type cluster with the centre fully occupied by a nickel atom. The nickel atom is surrounded by 12 titanium atoms at 2.78 Å, making a nearly undistorted icosahedron. A larger, second-shell, icosahedron is filled with 12 titanium/zirconium atoms. The numbers and average distances of nearest neighbours are summarized in table 1. All distributions of distances are broad. Around a titanium or a zirconium atom, there are nickel, titanium and zirconium neighbours. Around nickel, there are, on average, 2.8 titanium first neighbours located at a well-defined distance of 2.44 Å and 2.8 titanium atoms at a mean distance of 2.73 Å, plus a few more zirconium neighbours at distances beyond 3 Å. No nickel first neighbours are found around a nickel atom and the shortest Ni–Ni distance is greater than 5 Å. The well-defined Ni–Ti distance of 2.44 Å does not belong to the Ti icosahedron surrounding a nickel atom. Conversely, the 2.78 Å Ni–Ti distance in the Ti icosahedron appears outside the Ti icosahedron (2.71 Å). Most average interatomic distances have values near the sum of the atomic radii (Ti: 1.47 Å, Zr: 1.60 Å, Ni: 1.24 Å). However, the first Ti–Ni correlation, 2.46 Å, is clearly shorter than the sum of the atomic radii of Ti and Ni (2.71 Å). Also, the Zr–Ni (Ni–Zr) mean distance, 3.19 Å, is greater than the sum of the atomic radii of Zr and Ni (2.84 Å).

EXAFS spectra of this 1/1 Ti–Zr–Ni phase were successfully reconstructed using this model [7]. The average distances determined by EXAFS differ by less than 0.10 Å from the diffraction results. It should be kept in mind that the distributions of distances are very broad

Table 1. First environments in 1/1 $Ti_{50}Zr_{35}Ni_{15}$, 3/2 $Ti_{40}Hf_{40}Ni_{20}$ and amorphous $Ti_{25}Hf_{50}Ni_{25}$ alloys. For the EXAFS data, $\Delta R = \pm 0.06$ Å and $\Delta\sigma = \pm 0.06$ Å. The diffraction data are taken from Hennig *et al* [19], $\bar{R}$ is the average of several interatomic distances.

Central atom	1/1 $Ti_{50}Zr_{35}Ni_{15}$ Diffraction (19)		3/2 $Ti_{40}Hf_{40}Ni_{20}$ EXAFS (9, 10)		Amorphous $Ti_{25}Hf_{50}Ni_{25}$		
	N	$\bar{R}$ (Å)	R (Å)	σ (Å)	N	R (Å)	σ (Å)
Zr/Hf	8 Ti	3.07	3.05	0.11	3.8 Ti	2.87	0.23
	2.75 Ni	3.19	3.24	0.11	3.8 Ni	3.01	0.11
	4.5 Zr/Hf	3.27	3.35	0.18	7.6 Hf	3.27	0.16
Ti	1 Ni	2.44	2.48	0.11	3 Ni	2.47	0.20
	1 Ni	2.73	2.78	0.07			
	4.9 Ti	2.90	2.90	0.21	3 Ti	2.97	0.20
	5.1 Zr/Hf	3.07	3.01	0.12	6 Hf	2.97	0.12
Ni	2.8 Ti	2.44	2.49	0.11	2.8 Ti	2.46	0.12
					2.8 Ni	2.58	0.11
	2.8 Ti	2.73	2.68	0.13			
	5.6 Zr/Hf	3.19	3.19	0.14	5.6 Hf	2.97	0.17

in the 1/1 phase, which does not allow a precise determination of the distances by EXAFS. The same values of the interatomic distances were recovered for the heterogeneous pairs, from different edges, within about ±0.06 Å, which was taken to be the error for R and σ. This structural modelling of the 1/1 Ti–Zr–Ni phase was used to simulate the EXAFS spectra of the icosahedral Ti–Zr–Ni phase [7, 8] and of the 3/2 Ti–Hf–Ni alloy [9], substituting zirconium by hafnium. The number, N_j, of nearest neighbours was fixed to the values found in the model of the 1/1 phase, while the distances, R, and the disorder parameter, σ, were adjusted to fit the calculated spectra to the experimental data. The values obtained for the 3/2 phase are given in table 1. The local structure is very similar in the Ti–Zr–Ni alloys, quasicrystal or crystal, and in the 3/2 Ti–Hf–Ni phases, even around the zirconium/hafnium atoms. Therefore, some icosahedral ordering exists around nickel atoms in all these alloys. The first distance between titanium and nickel atoms (2.48–2.49 Å, in the 3/2 alloy), outside the Ti icosahedron, is very close to that in crystalline fcc Ti_2Ni (2.49 Å) [21, 22], where the distances between nickel atoms (2.87 Å) is greater than in pure nickel (2.49 Å). The close Ti–Ni approach indicates a tendency towards covalent bonding. The titanium atoms are at the same distance (2.90 Å) in the 3/2 Ti–Hf–Ni and in Ti_2Ni crystals. This distance is very near that in pure titanium (2.93 Å). The Hf–Ni correlation (3.19 Å) is noticeably greater than the sum of the atomic radii (2.82 Å). Upon hydrogenation [9], this Hf–Ni distance decreases drastically, while all of the other average distances increase, in line with the increase of the lattice parameter.

4. Non-hydrogenated alloy

A first attempt at modelling the local order of the non-hydrogenated amorphous alloy based on the local structure of the 3/2 phase could not give a coherent fit on the three edges, i.e. the same distances for heterogeneous pairs. Although the EXAFS spectra of the 3/2 and amorphous alloys are sufficiently similar for the Hf and Ti edges, the discrepancies for the Ni edge imply that the local order is not the same in the two alloys. In fact, the 10–15% variation of the Hf/Ti concentration leads to relative variations as high as 25–37.5% in going from the 3/2 alloy to the amorphous one. Therefore, the number, N_j, of nearest neighbours in the different subshells

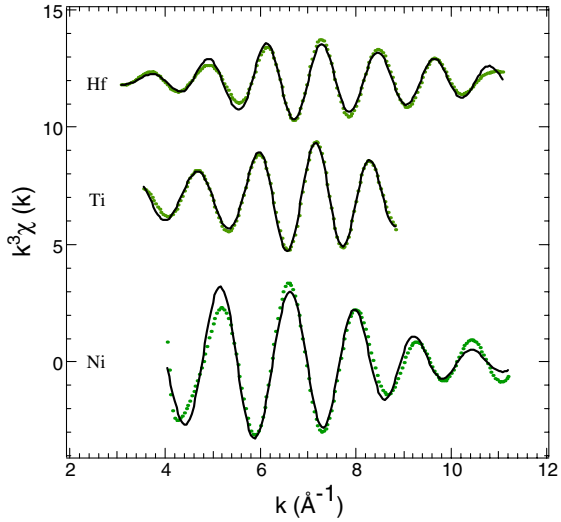

Figure 5. Fourier-filtered first shell of amorphous $Ti_{25}Hf_{50}Ni_{25}$ for the Hf L_{III}, Ti K and Ni K edges. Dots: experiment; curves: calculations.

can be different in the 3/2 and amorphous alloys. Moreover, homogeneous pairs do exist in the local environments of the metallic amorphous alloys, as for example in $Ni_{64}Zr_{36}$ [23, 24] or in $Zr_{70}Ni_{30}$ [25]. Therefore, the possibility of Ni–Ni pairs cannot be dismissed. Three subshells of Hf, Ti and Ni atoms were assumed around each type of atom. To minimize the number of parameters, the average total number of atoms neighbouring a central one was assumed to be the same as in the 1/1 model, but these atoms were distributed into the three Hf, Ti and Ni subshells according to the concentration of the elements in $Ti_{25}Hf_{50}Ni_{25}$. Around a nickel atom, this yields the same coordination numbers in the two crystalline and amorphous phases, with the second Ti subshell in the 3/2 phase becoming an Ni subshell in the glass, with Ni atoms substituting for Ti atoms. N_j and σ_j are correlated parameters in equation (1) and the σ_j parameters could, possibly, take into account some inaccuracy into the determination of N_j. For example, a change in σ_j can balance a variation of N_j.

These coordination numbers, N, and also the distances, R, and the disorder parameter, σ, used to simulate the Fourier-filtered spectra are given in table 1 and the fits are shown in figure 5. There is a good correlation of the distances obtained from the different edges for the heterogeneous pairs: Ni–Ti/Ti–Ni (2.46/2.47 Å), Ni–Hf/Hf–Ni (2.97/3.01 Å), Hf–Ti/Ti–Hf distance (2.87/2.97 Å). This leads to an inaccuracy of ±0.05 Å, below the error $\Delta R = \pm 0.06$ Å. The Hf–Ni correlation (3.01 Å) is noticeably shorter than in the 3/2 phase (3.24 Å), where it decreases upon hydrogenation towards 3.01 Å [9], i.e. the same value as in the amorphous phase. A remarkable feature is the existence of an Ni–Ni correlation at 2.58 Å, so the neighbourhood of a nickel atom is very similar to that in Ti_2Ni, with Hf substituting for Ti and also Ni. In fact, in Ti_2Ni, each nickel atom is surrounded by three nickel atoms, at 2.87 Å, and nine nearest neighbour titanium atoms, at distances 2.49, 2.57 and 2.91 Å. These neighbours form an irregular icosahedron around a nickel atom as shown in figure 6. The same seems to hold true for the amorphous phase, with approximately three titanium atoms at 2.46 Å, three nickel atoms at 2.58 Å and six hafnium atoms at 2.97 Å. The short Ni–Ti distance (2.46 Å) appears, in the amorphous phase, in the icosahedron around Ni atoms. This particular environment around a nickel atom explains the discrepancies observed in the spectra of the 3/2 and amorphous phases for the Ni edge.

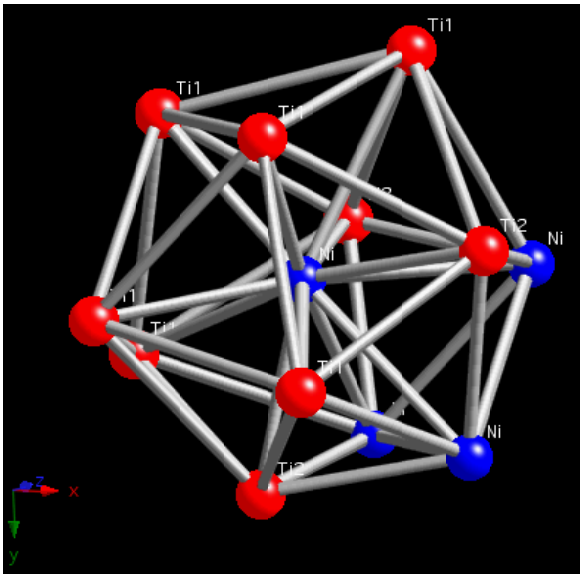

Figure 6. Icosahedral environment of a nickel atom in Ti_2Ni. Blue (dark grey) balls: nickel atom, red (light grey) balls: titanium atoms.

This new icosahedral atomic configuration found in the glassy Ti–Hf–Ni alloy around the nickel atoms mimics that found in the Ti_2Ni phase. Upon annealing at high temperatures, the glass, and the 3/2 approximant, transform to the Ti_2Ni-type phase [4, 12]. Some seeds of this structure likely pre-exist in the glass. Very recent results obtained in undercooled liquids [26] show the significant development of icosahedral order in supercooled liquids of Ni and Ti–Zr–Ni. The icosahedral arrangement becomes distorted in Ti, and Zr liquids and in Ti–Zr–Ni, as the Ni concentration is increased above 21%. For the 3/2 and glassy Ti–Hf–Ni alloys, the Ni concentrations are respectively 25 and 20%, so some structural transition could occur in this concentration range, if the short range order in the undercooled liquid can dictate the phases that form and the local order.

5. Hydrogenated alloys

The spectra of the hydrogenated amorphous alloys were simulated from the model of the non-hydrogenated one, keeping constant the numbers, N_j, of nearest neighbours, assuming that the mean coordination numbers remain unchanged upon hydrogenation. The distances, R, and the disorder parameters, σ, were allowed to vary. The values used to simulate the Fourier-filtered spectra are given in table 2 and the fits are shown in figure 7. They are very similar for the two hydrogenated alloys, as are the spectra, so there is not a clear distinction between samples containing H/M values of 1.2 and 1.4, contrary to the case of the 3/2 phase.

Around a nickel atom, the R-values do not change much, like the spectra, and the local environment does not seem much perturbed upon hydrogenation. Therefore, the local icosahedral configuration, similar to that in Ti_2Ni, is retained, although no peak corresponding to a crystalline phase, in particular to Ti_2Ni, appears in the XRD. Around a hafnium atom, the Hf–Ti and Hf–Hf correlations increase from respectively 2.87 to 3.17 Å (+0.20 Å) and 3.27 to 3.40 Å (+0.13 Å). The increase in the Hf–Ti distance is correlated with the Ti–Hf one,

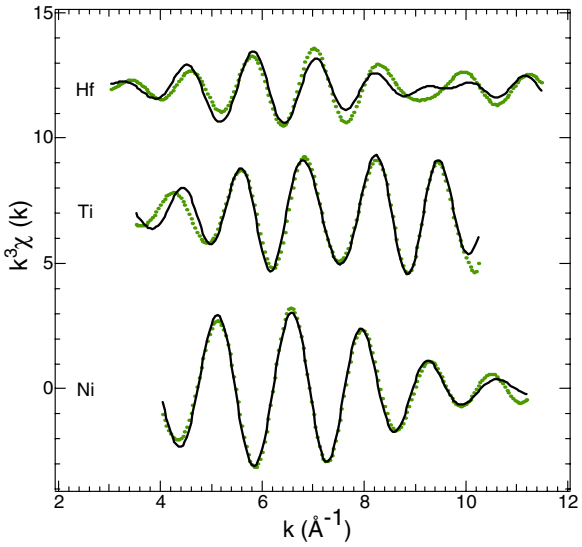

Figure 7. Fourier-filtered first shell of hydrogenated amorphous $Ti_{25}Hf_{50}Ni_{25}$ for the Hf L_{III}, Ti K and Ni K edges and for H/M = 1.25. Dots: experiment; curves: calculations.

Table 2. First environments in amorphous Ti–Hf–Ni and Ti–Hf–Ni:H alloys. $\Delta R = \pm 0.05$ Å and $\Delta\sigma = \pm 0.04$ Å.

H/M		0		1.2		1.4	
Central atom	N	R (Å)	σ (Å)	R (Å)	σ (Å)	R (Å)	σ (Å)
Hf	3.8 Ti	2.87	0.23	3.17	0.09	3.17	0.09
	3.8 Ni	3.01	0.11	2.97	0.11	2.97	0.10
	7.6 Hf	3.27	0.16	3.40	0.18	3.40	0.18
Ti	3 Ni	2.47	0.20	2.55	0.14	2.53	0.15
	3 Ti	2.97	0.20	2.91	0.10	2.90	0.12
	6 Hf	2.97	0.12	3.25	0.15	3.23	0.16
Ni	2.8 Ti	2.46	0.12	2.50	0.13	2.50	0.14
	2.8 Ni	2.58	0.11	2.56	0.13	2.55	0.13
	5.6 Hf	2.97	0.17	3.00	0.17	2.99	0.17

from 2.97 to 3.25 Å (+0.28 Å). Since the Hf–Ni correlation is almost constant, this yields an inversion of the titanium and nickel subshells around a central hafnium atom. This remarkable effect was already observed in the 3/2 phase, and also around zirconium, in the Ti–Zr–Ni alloys.

For the Ni edge, where the spectra are the most modified with hydrogenation in the 3/2 phase, the Ni spectra are similar for the hydrogenated 3/2 and amorphous phases. They were, however, analysed from the two different non-hydrogenated models, i.e. the W phase for the 3/2 approximant and the new icosahedral model for the glass. For the 3/2 phase, the σ-values are greater than 0.20 Å for the Hf and second Ti subshells, so that these subshells contribute little to the spectra, which is dominated by the first Ti subshell at about 2.55 Å. In the glass, the σ-values are smaller than 0.20 Å for all distances, and particularly less than 0.15 Å for the Ti and Ni subshells at 2.50–2.55 Å. Therefore, in the two phases, the Ni spectra are dominated by the Ti/Ni subshells at 2.50–2.55 Å, so that the local order appears to be similar in both phases.

Moreover, from the increase of the σ-values for the Ni–Ti/Hf bonds in the 3/2 phase [9], we can also infer that these bonds become weaker with hydrogenation and that Ni could possibly substitute for Ti around the Ni atoms in the 3/2 phase, leading to a local order similar to that in the glass around the Ni atoms.

The σ disorder parameter related to the Hf–Ti correlation decreases drastically upon hydrogenation, from 0.23 to 0.09 Å. Since the perturbation is a maximum for the Hf–Ti correlation, this suggests that the hydrogen atom resides near the hafnium and titanium atoms, pushing them apart. As a matter of fact, their distance, 3.17 Å, increases upon hydrogenation and becomes greater than the sum of the atomic radii of hafnium and titanium atoms, 3.05 Å (Hf: 1.58 Å, Ti: 1.47 Å). The experiments were made at low temperature, so the disorder parameter is mainly due to the structural disorder. The strong decrease in the σ parameter implies that the local distribution of atomic distances narrows, showing a higher degree of ordering of hafnium and titanium atoms. As the samples are fully charged with hydrogen (H/M = 1.2 and 1.4), this could be due to some strong correlation between hydrogen atoms, i.e. an H–H repulsive interaction, leading to some H network or skeleton, which could stiffen the whole structure.

The evolution of the local order upon hydrogenation is not exactly the same as in the 3/2 phase and in the Ti–Zr–Ni alloys, where significant changes in all the distances were observed. However, the perturbation of the neighbourhood due to hydrogenation is a maximum around the hafnium and titanium atoms in all these alloys and, consequently, hydrogen atoms sit preferentially near hafnium and titanium neighbours. Nevertheless, the change upon hydrogenation is somewhat smaller in the amorphous matrix, which could adapt more easily to the hydrogen atoms than the crystalline one, where symmetry rules must be satisfied.

6. Conclusions

EXAFS measurements were made in order to study the influence of hydrogen on the local structure of an amorphous Ti–Hf–Ni alloy, and to compare the behaviour to that found previously in the 3/2 approximant phase. Hydrogen concentrations of H/M = 1.2 and 1.4 were studied. The local structure was found to be different in the non-hydrogenated crystalline phase and in the amorphous phase, where a new icosahedral ordering, similar to that in the Ti_2Ni phase, was found around the nickel atoms.

In the hydrogenated amorphous alloys, the local order is similar for the 1.2 and 1.4 H/M ratio. As in the 3/2 phase and in the Ti–Zr–Ni alloys, the perturbation of the local structure concerns mainly the environments of hafnium (zirconium) and titanium atoms. Therefore, hydrogen atoms sit preferentially near hafnium (zirconium) and titanium neighbours. The neighbourhood of a nickel atom did not change appreciably with hydrogenation, contrary to its evolution in the 3/2 phase and in the Ti–Zr–Ni alloys. The local icosahedral environment, similar to that in the Ti_2Ni phase, is kept into the hydrogenated amorphous phase. Moreover, the similarity of the spectra for the Ni edge in the 3/2 and glassy phases suggests that the local order around the Ni in the 3/2 phase could evolve to that in the glass, with Ni atoms possibly substituting for Ti ones around Ni. Finally, a remarkable decrease of the disorder parameter for the Hf–Ti correlation in the glass could be due to a stiffening of the structure due to the formation of an hydrogen skeleton.

Acknowledgments

We are pleased to thank J Moscovici for his help during the EXAFS experiments. KFK gratefully acknowledges the support of the National Science Foundation under grant DMR 03-07410. AS dedicates this paper to the memory of Dale Sayers, a founder of the EXAFS

spectroscopy, who passed away on 25 November 2004 and who studied 'lots of stuff with XAFS'.

References

[1] Kelton K F, Kim W J and Stroud R M 1997 *Appl. Phys. Lett.* **70** 3230
[2] Kelton K F and Gibbons P C 1997 *Mater. Res. Soc. Bull.* **22** 69
[3] Viano A M, Stroud R M, Gibbons P C, McDowell A F, Conradi M S and Kelton K F 1995 *Phys. Rev.* B **51** 12026
[4] Huett V T and Kelton K F 2002 *Phil. Mag. Lett.* **82** 191
[5] Gratias D, Quiquandon M and Katz A 2000 *Quasicrystals Current Topics* ed E Belin-Ferré, C Berger, M Quiquandon and A Sadoc (Singapore: World Scientific) pp 1–72
[6] Maeland A J 1978 Comparison of hydrogen absorption in glassy and crystalline structures *Hydrides for Energy Storage* ed A F Andresen and A J Maeland (Oxford: Pergamon) pp 447–62
[7] Sadoc A, Kim J Y and Kelton K F 2001 *Phil. Mag.* A **81** 2911
[8] Sadoc A, Majzoub E H, Huett V T and Kelton K F 2002 *J. Phys.: Condens. Matter* **14** 6413
[9] Sadoc A, Huett V T and Kelton K F 2003 *J. Phys.: Condens. Matter* **15** 7469
[10] Sadoc A, Huett V T and Kelton K F 2004 *Mater. Res. Soc. Symp. Proc.* **805** 357
[11] Sadoc A, Huett V T and Kelton K F 2004 *LAM 12*; *J. Non-Cryst. Solids* submitted
[12] Huett V T and Kelton K F 2002 *Appl. Phys. Lett.* **81** 1026
[13] Kim J Y, Majzoub E H, Gibbons P C and Kelton K F 1999 *Mater. Res. Soc. Symp. Proc.* **553** 483
[14] Kim J Y, Gibbons P C and Kelton K F 1998 *J. Alloys Compounds* **266** 311
[15] Michalowicz A 1991 EXAFS pour le MAC *Logiciels pour la Chimie* (Paris: Société Française de Chimie) p 102
[16] Michalowicz A 1997 *J. Physique Coll.* **7** C2 235
[17] Stern E A, Sayers D E and Lytle F W 1975 *Phys. Rev.* B **11** 4836
[18] McKale A G, Veal B W, Paulikas A P, Chan S K and Knapp G S 1988 *J. Am. Chem. Soc.* **110** 3763
[19] Hennig R G, Majzoub E H, Carlsson A E, Kelton K F, Henley C L, Misture S, Kresse G and Hafner J 2000 *Proc. 7th Int. Conf. on Quasicrystals* ed F Gähler, P Kramer, H-R Trebin, K Urban; *Mater. Sci. Eng.* A **294/295** 361
[20] Kim W J, Gibbons P C, Kelton K F and Yelon W B 1998 *Phys. Rev.* B **58** 2578
[21] Yurko G A, Barton J W and Parr J G 1959 *Acta Crystallogr.* **12** 909
[22] Mueller M H and Knott H W 1963 *Trans. Met. Soc. AIME* **227** 674
[23] Lefebvre S, Quivy A, Bigot J, Calvayrac Y and Bellisent R 1985 *J. Phys. F: Met. Phys.* **15** L99
[24] Sadoc A and Calvayrac Y 1986 *J. Non-Cryst. Solids* **88** 242
[25] Saida J, Matsubara E and Inoue A 2003 *Mater. Trans.* **44** 1971
[26] Kelton K F, Gangopadhyay A K, Kim T H and Lee G W 2004 *LAM 12*; *J. Non-Cryst. Solids* submitted